Associative Behavior-Based abundance Index (ABBI) for western Indian Ocean bigeye tuna (*Thunnus obesus*) obtained from echosounder buoys data.

Yannick Baidai[1], Laurent Dagorn[2], Daniel Gaertner[2], Jean-Louis Deneubourg[3], Antoine Duparc[2], Laurent Floch[2], and Manuela Capello[2]

ABSTRACT

This paper presents the estimates of bigeye tuna (*Thunnus obesus*) abundance assessed from the associative behavior-based abundance index (ABBI). Taking advantage of the associative behavior of species around floating objects (FOBs) and acoustic data collected by echosounder buoys used in the tropical tuna purse seine fishery, the ABBI approach index allows for direct and effort-independent abundance estimates of tropical tuna species. Its implementation in the western Indian Ocean on small bigeye tuna (individual less than 10 kg) has shown a decline in abundance of this species since 2018, relative to the reference levels of 2013.

Keywords: *Abundance Index; Associative behavior; FADs; Bigeye tuna*

1. INTRODUCTION

Traditionally caught by the longline fleet operating in the region, a significant portion of catches of bigeye tuna (*Thunnus obesus*) is nowadays carried out by the purse seine fleets at drifting fish aggregating devices (DFADs). Defined as man-made floating objects, specifically designed to attract and concentrate tunas, DFADs are typically equipped with tracking technology (GPS) and echosounder buoys to remotely detect the associated tuna biomass and their location (Lopez *et al*., 2014). DFADs have considerably increased the catchability of tropical tuna species, notably juveniles of yellowfin and bigeye tuna, and are considered as one of the most important changes that have contributed to the increase in the efficiency of purse seiners (Fonteneau *et al*., 2013). However, the non-random nature of this fishing method has significantly complicated the estimation of fishing effort in the purse seine fishery and, consequently, the

---

[1] African Marine Expertises, Abidjan, Côte d'Ivoire
[2] MARBEC, Univ Montpellier, CNRS, Ifremer, IRD, Sète, France
[3] Unit of Social Ecology, Université Libre de Bruxelles (ULB), Bruxelles, Belgium

standardization of CPUE abundance indices from purse-seine bigeye tuna catches obtained from DFAD-associated schools.

Recently, the availability to scientists of new data obtained from electronic tagging and/or echosounder buoys has allowed the development of alternative methods for deriving abundance indices for tropical tuna populations (Capello *et al.*, 2016; Santiago *et al.*, 2020; Baidai *et al.*, 2021). Within this perspective, this work addresses the population assessment of small bigeye tuna (i.e., individuals under 10 kg) in the western Indian Ocean, based on a dedicated methodology which exploits the associative behavior of this species, quantified using data from echosounder buoys attached to DFADs and electronic tagging experiments, in order to derive direct and effort-independent abundance estimates: the Associative Behavior-Based abundance Index (ABBI).

2. MATERIALS AND METHODS

2.1. Model definition

The associative behaviour of tropical tuna implies that tuna schools can be in two states, either associated with FOBs, or not associated, i.e., in the so-called free-swimming state. At any given time t, the overall abundance of tuna (N) in a given area results from the sum of the abundances of two components: the associated (X_a) and the free-swimming populations (X_u).

$$N(t) = X_a(t) + X_u(t) \tag{1}$$

Within a given study region and time period, the average associated tuna population ($\overline{X_a}$) can be estimated as follows:

$$\overline{X_a} = \bar{m}\bar{f}\bar{p} \tag{2}$$

Where $\bar{m}$ is the average tuna biomass estimated under FOBs occupied by tuna aggregation, $\bar{f}$ represents the average proportion of FOBs with tuna aggregations and $\bar{p}$ the average number of FOBs in the region of interest.

Capello *et al.*, (2016) demonstrated that the ratio between the average size of the associated component to the total population can be estimated by measuring the uninterrupted period of time that tunas spend either associated with, or disassociated from a FOB, i.e., the average continuous residence time (CRT) and the average continuous absence time (CAT):

$$\frac{\overline{X_a}}{\overline{N}} = \frac{CRT}{CRT + CAT} \quad (3)$$

Because the amount of time that tuna spends associated at FOBs (or out of them) can be species and size-dependent (Dagorn *et al.*, 2007; Robert *et al.*, 2012), Equation (3) is valid for tuna species and size classes that manifest the same associative behavior with FOBs. In the following, we will consider small (individual under 10 kg) bigeye tuna whose associative behaviour with FOBs has been studied within acoustic tagging experiments within arrays of drifting and anchored FADs (Table 1).

Considering Equations (2-3), the total tuna population within an area can be estimated as:

$$\overline{N} = \frac{CRT + CAT}{CRT}\overline{m}\bar{f}\bar{p} \quad (4)$$

Furthermore, considering Equations (1 – 2) and (4), the free-swimming population (X_u) can be expressed from the following relation:

$$\overline{X_u} = \frac{CAT}{CRT}\overline{m}\bar{f}\bar{p} \quad (5)$$

2.2. Study area and period

The study area extended over the western Indian Ocean, between latitudes 10° S and 10° N and covered longitudes located between the eastern African coasts and 70° E (Figure 1). The abundance estimates were conducted in between 2013 and 2019, using a spatio-temporal stratification of 10°×10° and quarter-year (Figure 1).

2.3. Field data

2.3.1. Total number of floating objects (p)

The number of FOBs in each of the time-area units was assessed from the number of buoys equipping the DFADs deployed by the French tuna purse seine fleet, and two raising factors. First, the estimates of the total number of DFADs were calculated from the ratios between DFADs deployed by French and Spanish purse-seiners fleets, provided from 2010 to the end of 2017, by Katara *et al.* (2018). The missing ratios for the years 2018 and 2019 were estimated using the average ratio over the year 2017, based on the assumption of a relative stabilization in the exploitation of buoys between the different fleets after this period (limitation measures on the number of buoys operated by tuna purse-seiners in the Indian Ocean: IOTC Resolutions 15/08 and 17/08). The total number of FOBs in each time-area unit was then derived from the ratios of DFADs encountered by observers on-board French tuna seiners, relative to other natural (marine mammals, trees, etc.) or artificial (debris from human activities) floating objects (Figure 2). This ratio was derived from observers' data collected under the EU Data Collection Framework (DCF) and the French OCUP program (Observateur Commun Unique et Permanent), with an overall average coverage rate of about 50% over the years 2013 to 2017 (Goujon *et al.*, 2017).

2.3.2. FOB-associated average tuna biomass (m)

The average biomass of small bigeye tuna (i.e. less than 10 kg) , referred to as BET(<10kg), around an inhabited FOB (i.e., a FOB occupied by a tuna aggregation) in the study area was derived from purse seine catches at DFAD made by the French fleet as well as data from port sampling programs (Table 2). To this purpose, the DFAD-catches reported in vessel logbooks were corrected using the T3 processing (Pallarés et Petit, 1998; Duparc *et al.*, 2018). The catch corrections firstly involve adjusting the catches from the logbook, using the weights reported in the landing notes, in order to overcome biases in catch data reported by skippers.

Then, because species composition of all sets could not be known exactly, average species compositions were derived from sampling data from tuna purse seine catches at DFADs during landing, in accordance with level 2 of the T3 processing (see details in Duparc *et al.*, 2018). During this step, the length-weight relationships, with official IOTC parameters (Chassot *et al.*, 2016) were used for each species. Species compositions were then averaged by stratum, with a minimum threshold of 20 available data points (sampled sets) per strata.

Where species composition values were missing for a given stratum, they were generated using their corresponding least-squares means in a reference grid as described by Lenth (2016). The reference grid consists of the set of all combinations of predictor levels (*i.e*. the time-area strata) and least-squares means were the prediction values from the species composition models. We assessed the species composition of sets using a zero-and one-inflated beta model. The proportion of the bigeye tuna in the set obtained from the sampling programs formed the response variable, while the year, quarter and spatial strata were predictors. All predictors were used to model the mean, variance, zero-inflated and one-inflated components of the model. Model selections were performed on each model component using a Generalized Akaike

Information Criterion. Diagnostics of the selected models were checked: the normalized quantile residuals against the fitted values and the case number (i.e. index number), together with their kernel density estimate and a normal Q-Q plot (Figure 3a).

Thereafter, catches per size category were finally calculated by multiplying the corrected logbook catches with the average composition calculated in the corresponding time-area stratum of the fishing set. Finally, the average biomass associated with a FOB (m) was calculated for each stratum from the corrected catches of small bigeye tuna, using the threshold procedure on the number of sets described above. The catch and species composition data provided by the Ob7 were collected under the Data Collection Framework (Reg. 2017/1004 and 2016/1251) funded by IRD and the European Union. The figure 4 provides the time series of the FOB-associated biomasses obtained from this protocol, for each of the three species, across the various spatial strata considered.

2.3.3. Proportion of inhabited FOBs (f)

Acoustic data collected by the Marine Instruments M3I buoys were translated into presence/absence of a tuna aggregation, using a machine learning algorithm (Baidai *et al.*, 2020), that was shown to provide good accuracies (85%) in the Indian Ocean. The first sections of presence or absence occurring at the beginning of the FAD trajectories were excluded from the analysis as they may result from the colonization period of the DFAD during which the DFAD-tuna system is not yet at equilibrium, or potentially from classification errors related to the operation on the buoy (Baidai *et al.*, 2020).

Daily presence/absence data were then used to derive the proportion of FOBs inhabited by a tuna aggregation (f). This was expressed as the number of DFADs (equipped by an M3I buoy) classified as inhabited by a tuna aggregation, divided by the total number of M3I buoys at a daily scale. A threshold of at least 10 available buoys per day and space-time unit was considered for the calculation of the daily proportion of inhabited FOBs. Table 2 provides the average daily numbers of available M3I buoys used over the study area. Quarterly averages of the proportion of inhabited FOBs were then calculated. Because an accurate species discrimination from these acoustic data was not possible, these values were corrected with the occurrence of small bigeye tuna (BET (<10 kg)) in the FOB-associated tuna aggregations, according to Equation (6):

$$f(\text{BET}(<10\text{ kg})) = f.\eta(\text{BET }(<10\text{ kg})) \qquad (6)$$

where $\eta(\text{BET}(<10\text{ kg}))$ represents the ratio between the number of DFAD-catches with a biomass of small bigeye tuna relative to the total number of positive DFAD catches (considering only DFAD catches with a total biomass greater than or equal to 1 tonne).. This ratio was estimated on a quarterly basis, within each grid cell, using the sampling data raised to the catch per set. A minimum number of 20 available sampling data per strata was considered for the ratio calculation. Missing occurrence values for a given stratum were estimated from a binomial model using year, quarter and spatial strata as predictors (Figure 3b). The time series of the estimated proportions of FOBs inhabited by small bigeye tuna are presented in the figure 5.

2.3.4. Time spent by tuna associated: Continuous residence time of bigeye tuna (CRT)

Tuna CRTs have been shown to vary according to their species, size (Ohta et Kakuma, 2005; Robert *et al.*, 2012, Rodriguez et al. 2017) and FOB density (Pérez *et al.*, 2020). Nevertheless, numerous studies across all tropical oceans have shown that the magnitude of these variations remains relatively small for the three tuna species and the life stages considered in this work (Dagorn *et al.*, 2007; Matsumoto *et al.*, 2014, 2016; Tolotti *et al.*, 2020; Govinden *et al.*, 2021). Considering this characteristic, a constant CRT value was assumed for small bigeye tuna in all spatial and temporal strata. The value was provided by Govinden et *al.* (2021), who measured an average CRT at DFADs for bigeye tunas of 7.6 ± 7.2 days.

2.3.5. Continuous absence time of yellowfin tuna (CAT)

Currently, CRTs around DFADs could be estimated through acoustic tagging for the three main tuna species (Dagorn *et al.*, 2007; Matsumoto *et al.*, 2014, 2016; Scutt *et al.*, 2019; Tolotti *et al.*, 2020; Govinden *et al.*, 2021). However, no direct measurement of tropical tuna CATs has yet been carried out on DFADs in the study area. Only experiments conducted on anchored FAD arrays could estimate CATs so far. Recent studies demonstrated decreasing CATs for increasing numbers of FOBs (Rodriguez-Tress *et al.*, 2017; Pérez *et al.*, 2020). An intuitive argument that explains how the time spent by tuna between two FOB associations (the CAT) depends on the FOB densities, relies on the fact that the FOB encounter rates by a tuna are smaller (i.e., larger CATs) when the distances between FOBs are larger (i.e., smaller FOB densities). From these findings, the CAT was related to the number of FOBs according to the following ansatz:

$$CAT = \frac{1}{\phi p} \quad (7)$$

where ϕ is a parameter that depends on the probability to associate to one of the p FOBs. The associative processes of a tuna can realistically concern only a limited number of FOBs (p_0) relative to those present in the large spatial strata considered in this study (p). This p_0 represents the local number of FOBs likely to be visited by the tuna in its local environment, *i.e.*, those located in the area S_0 explored by the tuna between two consecutive FOB associations and thus which may be locally encountered by the tuna following its departure from another FOB. Assuming that within this area (S_0) all FOBs have the same probability μ of being visited by tuna, the CAT definition can therefore be rewritten according to the following equation:

$$\overline{CAT} = \frac{1}{p_0 \mu} \quad (8)$$

Assuming a uniform FOB density results in:

$$\frac{p}{S} = \frac{p_0}{S_0} \quad (9)$$

where S represents the area considered for the abundance assessment in this study. Inserting the above relationship into the CAT definition provided in Equation 8 leads to:

$$\overline{CAT} = \frac{1}{\left(\frac{S_0}{S}\mu\right)p} \quad (10)$$

Considering the ansatz provided in Equation (7), it is possible to express the parameter ϕ as the product of the surface ratio and the association probability μ:

$$\phi = \frac{S_0}{S}\mu \quad (11)$$

In this respect, the ϕ parameter is intended to switch from the local scale at which associative processes take place (where a CAT occurs with probability $p_0\mu$), to the scale of oceanic regions considered for the abundance estimates (where the number of FOBs is estimated). The area S_0 depends on the search dynamics of tuna in a FAD array. It can be estimated using the theoretical area that a tuna could cover during the average time spent between two FOB associations. Considering a temporal scale of one day, *i.e.*, the typical time unit of CATs measured for tuna in FAD arrays(Pérez *et al.*, 2020), the upper bound for this area would correspond to a circle with radius equal to the maximum distance travelled by a tuna in 24 hours (the case of a "straight-line swim" to the FOB). For 50 cm tunas moving at a constant speed of one body length/second, the upper bound for the area S_0 would thus extend to about 6,000 km². Considering the approximately 1,2 million km² of the 10°×10° spatial strata, the surface ratio S_0/S would therefore approximate to 5e-3. Since μ (daily probability of associating) in equation (11) is naturally smaller than one, the value of this surface ratio provides the theoretical upper bound of ϕ for the stratification considered here. Assuming a random distribution of FOBs across spatial strata and considering the average density of FOBs of ~1700 FOBs per 10°×10° square (see Figure 2), the average distance between a FOB and its nearest neighbor can be estimated to be approximately 13 km. In order to evaluate the sensitivity of the ABBI index to different values of ϕ, a range of CATs from 10 to 30 days (corresponding to ϕ values between 2e-5 and 6e-5 from equation (6) for an average number of 1700 FOBs per 10°×10° square), were considered for the abundance assessments. The values in this range also provide consistent species-specific abundance estimates relative to the overall catches taken by all fishing gears targeting the three species in the study area and period, according to the IOTC catch database (https://www.iotc.org/data/datasets). This database provides the catches and effort data by month, species and gear at varying spatial aggregations (e.g. 1°×1° grid area for purse seine and 5°×5° grid area for longline) on a flag state basis. Total catches for each of the three species were aggregated by 10°×10° square and quarter. Then, the catches of small individuals (fish under 10 kg) of bigeye tuna were calculated using the average species and weight composition calculated at the same stratification level used for the length-frequency samples provided in the IOTC database.

2.4. Abundance estimates

Abundance estimates were conducted considering a spatio-temporal stratification of 10° quarter. In each 10 ×10° grid cell, the associated, free-swimming and total BET-10kg abundance was calculated following respectively the Equations (2), (5) and (4). For each component (associated, free-swimming and total), an average quarterly index was then estimated for the full study area, considering the average over the spatial strata with available data for the same period. Relative abundance indices for the different components are also provided, considering the first quarter of the year 2013 as reference and different values of ϕ (for the total population).

3. Results and Discussion

3.1. Time series of abundance of small bigeye tuna (<10 kg) in the western Indian Ocean

Figures 6 and 7 show, respectively, the average estimates of absolute and relative abundance of the total population of small bigeye tuna (<10kg) calculated per 10°×10° square, and for its associated and free components. They reveal that globally both components of the BET (<10kg) population follow roughly similar trajectories throughout the study period. The result also highlighted a gradual decline in the abundance of all small bigeye tuna since 2018, with a depletion of more than to 60%, observed at the end of 2019.

The variation of the ϕ values used for the free-swimming and the total population did not change the trends of the estimated biomass qualitatively. Indeed, when examined in relative terms, the ABBI showed very low sensitivity to the values of the parameter (ϕ) used in setting the ranges of CAT. However, the variability of the absolute ABBI estimates remained closely linked to the ranges of CAT used. For average CATs, expected to be between 10 and 30 days (corresponding to ϕ values of 6e-5 and 2e-5), the ABBI estimates indicate average biomasses of small bigeye tuna calculated over the entire period and study area between 1,200 ± 720 tonnes and 2,500 ± 1,400 tonnes.

From a set of descriptive metrics of the associative behaviour of tunas around floating objects (namely residence and absence times) and the occupancy rate of these objects by tuna aggregations, the ABBI approach thus provided direct, effort-independent and absolute abundance indices for small bigeye tuna (<10 kg) in the Western Indian Ocean. However, data collection was one of the main challenges that hindered its implementation. For instance, current collection of tuna continuous residence times (CRT) is usually related to short-term projects, and remains limited to specific oceanic regions and periods. Similarly, although the technology exists to allow for the measurement of tuna continuous absence time (*CAT*), this metric has so far received very little attention and there is currently a critical need of knowledge on this essential data to understand the associative behaviour of tuna (Dagorn *et al.*, 2007; Robert *et al.*, 2012, 2013; Rodriguez-Tress *et al.*, 2017). Additional efforts for regular and large-scale electronic tagging programs would be critical to provide a better understanding of the associative behavior of tunas, and to carry out accurate assessments of their populations based on the ABBI methodology.

Here the ABBI framework illustrates the important contribution that unconventional data sources and technologies such as electronic tagging and echosounder buoys can make towards improving the inputs in fish stock assessments. To date, the data required for this approach are mainly devoted to either improve general knowledge on the ecology of tuna species (behavioural metrics) or for commercial (acoustic monitoring of FADs deployed by purse seiners) or regulatory purposes (monitoring the number of FADs by regional fisheries management organizations). The possibility to derive abundance indices from these data using alternative approaches to CPUE-based methods could support future developments of dedicated data collection programs, and help improve tropical tuna stock assessments, and thus fisheries management.

ACKNOWLEDGEMENTS

This project is co-funded by the ANR project BLUEMED (ANR-14-ACHN-0002) and “Observatoire des Ecosystèmes Pélagiques Tropicaux exploités” (Ob7) from IRD/MARBEC. The authors would also like to thank ISSF for supporting the project. The authors are grateful to ORTHONGEL and its contracting parties (CFTO, SAPMER, SAUPIQUET) for providing the echosounder buoys data. The authors also thank all the skippers who gave time to share their experience and knowledge on the echosounder buoys. The authors sincerely thank the contribution of the staff of the Ob7 on the databases of the echosounder buoys. We are also deeply grateful to the buoy manufacturers for their useful advice and information on their echosounder buoys.

REFERENCES

Baidai, Y., Dagorn, L., Amande, M. J., Gaertner, D., et Capello, M. 2020. Machine learning for characterizing tropical tuna aggregations under Drifting Fish Aggregating Devices (DFADs) from commercial echosounder buoys data. Fisheries Research, 229: 105613.

Baidai, Y., Laurent, D., Gaertner, D., Deneubourg, J. L., Duparc, A., Floch, L., et Capello, M. 2021. Associative Behavior-Based abundance Index (ABBI) for yellowfin tuna (Thunnus albacares) in the Western Indian Ocean. IOTC-2021-WPTT23(DP)-15_Rev1

Capello, M., Deneubourg, J. L., Robert, M., Holland, K. N., Schaefer, K. M., et Dagorn, L. 2016. Population assessment of tropical tuna based on their associative behavior around floating objects. Scientific Reports, 6: 36415.

Chassot, E., Assan, C., Esparon, J., Tirant, A., Delgado de Molina, A., Dewals, P., Augustin, E., *et al.* 2016. Length-weight relationships for tropical tunas caught with purse seine in the Indian Ocean : update and lessons learned. WPDSC12-INF05.

Dagorn, L., Pincock, D., Girard, C., Holland, K., Taquet, M., Sancho, G., Itano, D., *et al.* 2007. Satellite-linked acoustic receivers to observe behavior of fish in remote areas. Aquatic Living Resources, 20: 307-312.

Dagorn, L., Bez, N., Fauvel, T., et Walker, E. 2013. How much do fish aggregating devices (FADs) modify the floating object environment in the ocean? Fisheries Oceanography, 22: 147-153.

Duparc, A., Cauquil, P., Depetris, M., Dewals, P., Floch, L., Gaertner, D., Hervé, A., *et al.* 2018. Assessment of accuracy in processing purse seine tropical tuna catches with the T3 methodology using French fleet data: 1-19.

Fonteneau, A., Chassot, E., et Bodin, N. 2013. Global spatio-temporal patterns in tropical tuna purse seine fisheries on drifting fish aggregating devices (DFADs): Taking a historical perspective to inform current challenges. Aquatic Living Resources, 26: 37-48.

Goujon, M., Maufroy, A., Relot-Stirnemann, A., Moëc, E., Bach, P., Cauquil, P., et Sabarros, P. 2017. Collecting data on board French and Italian tropical tuna purse seiners with common observers: results of ORTHONGEL'S voluntary observer program OCUP (2013-2017) in the Indian ocean. IOTC-2017-WPDCS13-22_Rev1.

Govinden, R., Capello, M., Forget, F., Filmalter, J. D., et Dagorn, L. 2021. Behavior of skipjack (Katsuwonus pelamis), yellowfin (Thunnus albacares), and bigeye (T. obsesus) tunas associated with drifting fish aggregating devices (dFADs) in the Indian Ocean, assessed through acoustic telemetry. Fisheries Oceanography: fog.12536.

Grande, M., Capello, M., Baidai, Y., Uranga, J., Boyra, G., Quincoces, I., Orue, B., *et al.* 2020. From fishermen to scientific tools: progress on the recovery and standardized processing of instrumented buoys data. Collected Volume of Scientific Papers ICCAT, 76: 881-891.

Katara, I., Gaertner, D., Marsac, F., Grande, M., Kaplan, D., Agurtzane, U., Loreleï, G., *et al.* 2018. Standardisation of yellowfin tuna CPUE for the EU purse seine fleet operating in the Indian Ocean. IOTC–2018–WPTT20–36_Rev1.

Lenth, R. V. 2016. Least-Squares Means: The R Package lsmeans. Journal of Statistical Software, 69.

Lopez, J., Moreno, G., Sancristobal, I., et Murua, J. 2014. Evolution and current state of the technology of echo-sounder buoys used by Spanish tropical tuna purse seiners in the Atlantic, Indian and Pacific Oceans. Fisheries Research, 155: 127-137.

Matsumoto, T., Satoh, K., et Toyonaga, M. 2014. Behavior of skipjack tuna (Katsuwonus pelamis) associated with a drifting FAD monitored with ultrasonic transmitters in the equatorial central Pacific Ocean. Fisheries Research, 157: 78-85.

Matsumoto, T., Satoh, K., Semba, Y., et Toyonaga, M. 2016. Comparison of the behavior of skipjack (Katsuwonus pelamis), yellowfin (Thunnus albacares) and bigeye (T. obesus) tuna associated with drifting FADs in the equatorial central Pacific Ocean. Fisheries Oceanography, 25: 565-581.

Moniz, I., et Herrera, M. 2019. Using FADs to develop better abundance indices for tropical tuna. Collect. Vol. Sci. Pap. ICCAT, 75: 2196-2201.

Moreno, G., Boyra, G., Sancristobal, I., Itano, D., et Restrepo, V. 2019. Towards acoustic discrimination of tropical tuna associated with Fish Aggregating Devices. PLOS ONE, 14: e0216353.

Ohta, I., et Kakuma, S. 2005. Periodic behavior and residence time of yellowfin and bigeye tuna associated with fish aggregating devices around Okinawa Islands, as identified with automated listening stations. Marine Biology, 146: 581-594.

Pallarés, P., et Petit, C. 1998. Tropical tunas: new sampling and data processing strategy for estimating the composition of catches by species and sizes. Collect. Vol. Sci. Pap. ICCAT, 48: 230-246.

Pérez, G., Dagorn, L., Deneubourg, J. L., Forget, F., Filmalter, J. D., Holland, K., Itano, D., *et al.* 2020. Effects of habitat modifications on the movement behavior of animals: the case study of Fish Aggregating Devices (FADs) and tropical tunas. Movement Ecology, 8: 1-11.

Robert, M., Dagorn, L., Deneubourg, J. L., Itano, D., et Holland, K. 2012. Size-dependent behavior of tuna in an array of fish aggregating devices (FADs). Marine Biology, 159: 907-914.

Robert, M., Dagorn, L., Lopez, J., Moreno, G., et Deneubourg, J. L. 2013. Does social behavior influence the dynamics of aggregations formed by tropical tunas around floating objects? An experimental approach. Journal of Experimental Marine Biology and Ecology, 440: 238-243.

Rodriguez-Tress, P., Capello, M., Forget, F., Soria, M., Beeharry, S., Dussooa, N., et Dagorn, L. 2017. Associative behavior of yellowfin Thunnus albacares, skipjack Katsuwonus pelamis, and bigeye tuna T. obesus at anchored fish aggregating devices (FADs) off the coast of Mauritius. Marine Ecology Progress Series, 570: 213-222.

Santiago, J., Uranga, J., Quincoces, I., Orue, B., Merino, G., Murua, H., et Boyra, G. 2020. A novel index of abundance of juvenile yellowfin tuna in the Atlantic Ocean derived from echosounder buoys. Collect. Vol. Sci. Pap. ICCAT, 76: 321-343.

Scutt, P., Leroy, B., Peatman, T., Escalle, L., et Smith, N. 2019. Electronic tagging for the mitigation of bigeye and yellowfin tuna juveniles by purse seine fisheries. WCPFC-SC15-2019/EB-WP-08.

Tolotti, M. T., Forget, F., Capello, M., Filmalter, J. D., Hutchinson, M., Itano, D., Holland, K., *et al.* 2020. Association dynamics of tuna and purse seine bycatch species with drifting fish aggregating devices (FADs) in the tropical eastern Atlantic Ocean. Fisheries Research, 226: 105521.

Tables

Table 1: Summary of main findings from previous studies on bigeye tuna individual CRT assessed under an anchored and under an drifting FADs (FL: Fork length).

Study	Location	FL range (cm)	CRT
Dagorn *et al.*, (2007)	Western Indian Ocean	*Not provided*	Average at 1.43 days (maximum: 3.06 days)
Govinden *et al.*, (2021)	Western Indian Ocean	43 – 59	Average at 7.59 days (maximum: 16.49 days)
Matsumoto *et al.*, (2016)	Equatorial central Pacific Ocean	33.5 – 85.5	Average at 3.8 days (maximum: about 11 days)
Scutt *et al.*, (2019)	Western Central Pacific Ocean	37 – 90	Median at 10 days (maximum: 30 days)
Tolotti *et al.*, (2020)	Eastern Atlantic Ocean	45 – 61	Average at 25.31 days (maximum value to 55 days)

Table 2: Number of fishing sets and buoys used to estimate the average biomasses of small bigeye tuna and the proportions of floating objects with tuna aggregations, respectively. The "FOB sets" column indicates the total number of fishing sets on floating objects (FOBs) from the logbook data corrected with the T3 process. The "sampled FOB sets" column indicates the number of sampled fishing sets used to estimate the species compositions and occurrences in associated FOB aggregations. "M3I buoy count" and "Total buoy count" represent the daily average number of French M3I buoys and total number of French buoys in the study area by quarter.

Year	Quarter	FOB sets	Sampled FOB sets	M3I buoy count	Total buoy count
2013	Q1	171	49	329	424
	Q2	247	88	346	488
	Q3	406	112	492	689
	Q4	505	155	375	671
2014	Q1	321	78	327	745
	Q2	229	54	448	934
	Q3	472	130	516	984
	Q4	405	85	663	1126
2015	Q1	139	19	630	939
	Q2	154	16	993	1344
	Q3	360	70	1327	1620
	Q4	476	91	1487	1729
2016	Q1	334	67	1715	1940
	Q2	279	34	1705	1871
	Q3	531	116	1705	1832
	Q4	507	104	2092	2185
2017	Q1	283	32	2069	2223
	Q2	402	93	1717	2324
	Q3	529	132	2022	2841
	Q4	424	130	1925	2528
2018	Q1	547	143	1911	2366
	Q2	427	150	2004	2494
	Q3	540	200	2064	2690
	Q4	506	193	2184	2866
2019	Q1	426	138	1980	2807
	Q2	217	45	1780	2485
	Q3	428	97	1783	2507
	Q4	573	154	1722	2589

Figures

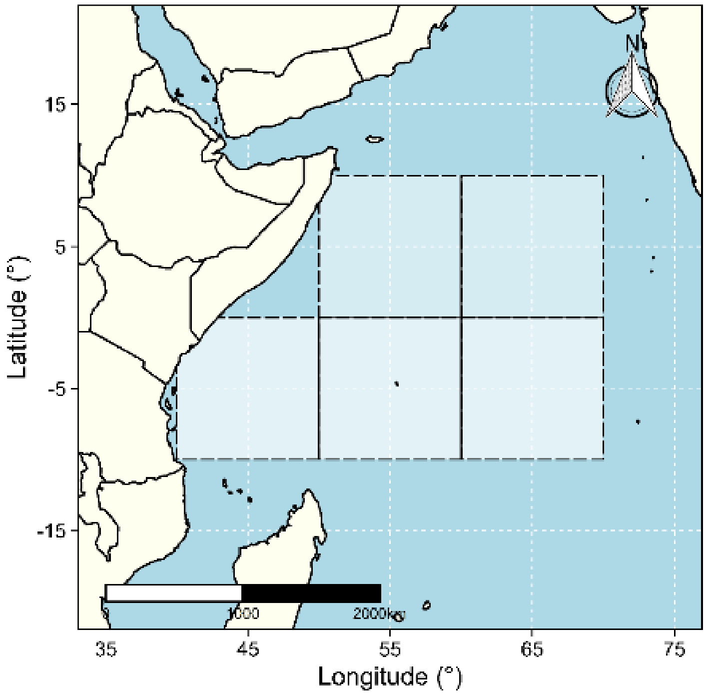

Figure 1: Spatial stratification of the study area

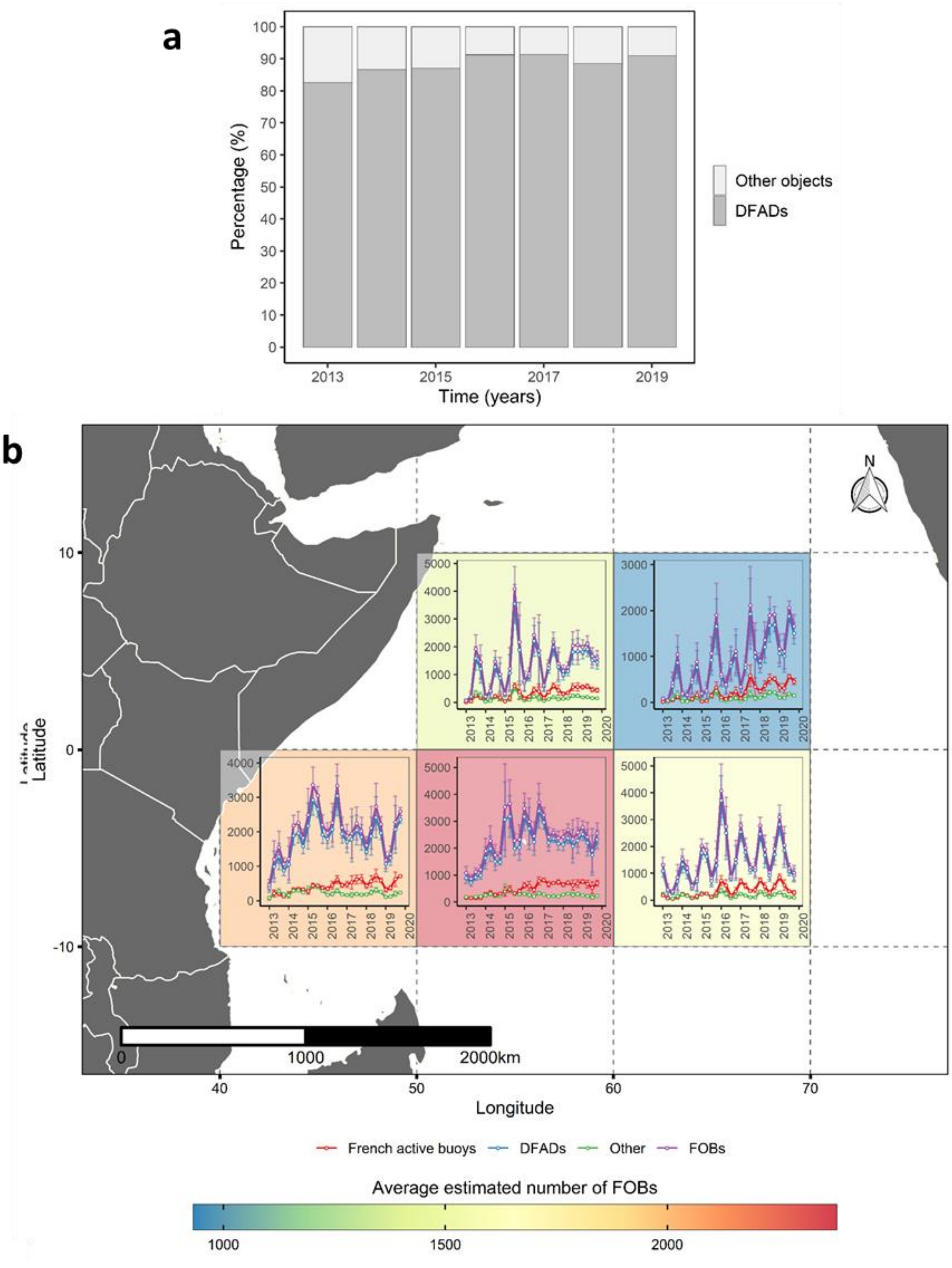

Figure 2: Estimates of the number of floating objects in the study area. (**a**), Percentage of drifting fish aggregating devices (DFADs) and other types of natural and artificial objects (Other objects) reported by observers on board French tuna purse-seiners. (**b**) Quarterly averages of the daily number of active buoys in the French fleet, the estimated numbers of drifting fish aggregating devices (DFADs), the other objects (Others), and the estimated total number of floating objects (FOBs = DFADs + Others) by 10° × 10° spatial strata in the western Indian Ocean. The background colors indicate the average number of FOBs calculated from 2013 to 2019 in each spatial stratum.

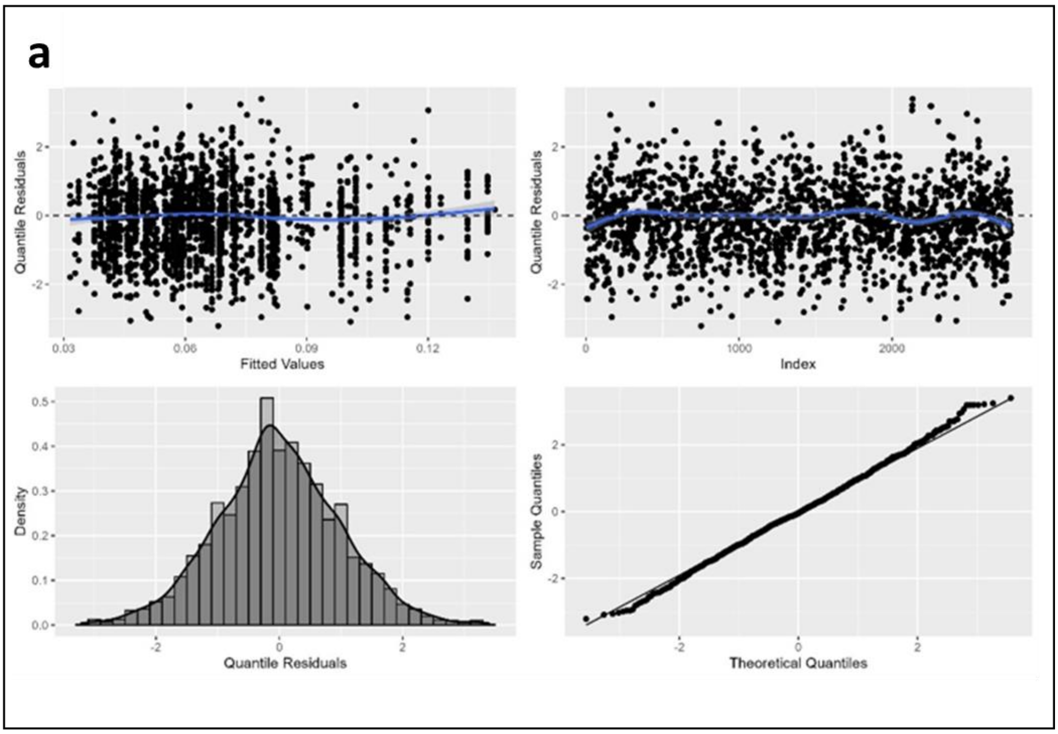

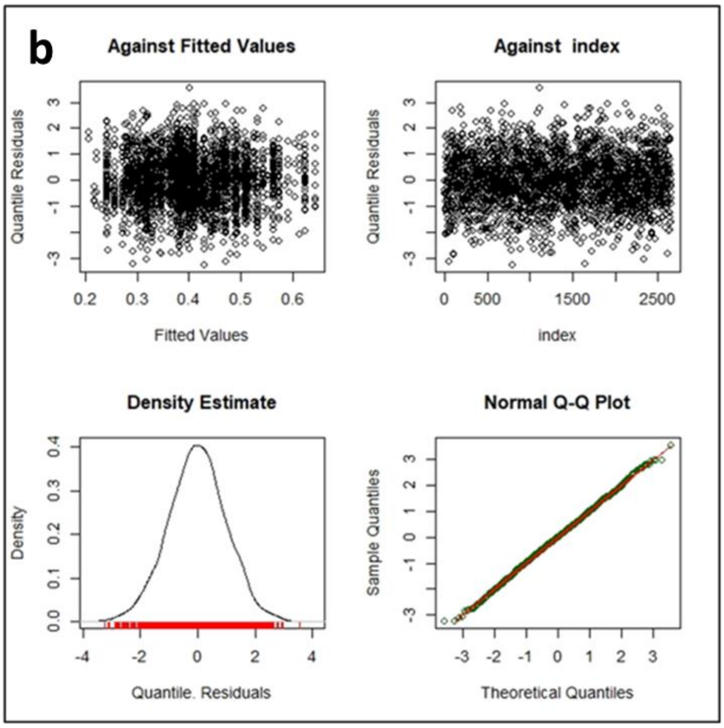

Figure 3: Residual diagnostic figures. (**a**) Zero and one-inflated beta models used to estimate missing composition values for small bigeye tuna (<10 kg), (**b**) Binomial model used to estimate missing occurrence values for small bigeye tuna (<10 kg).

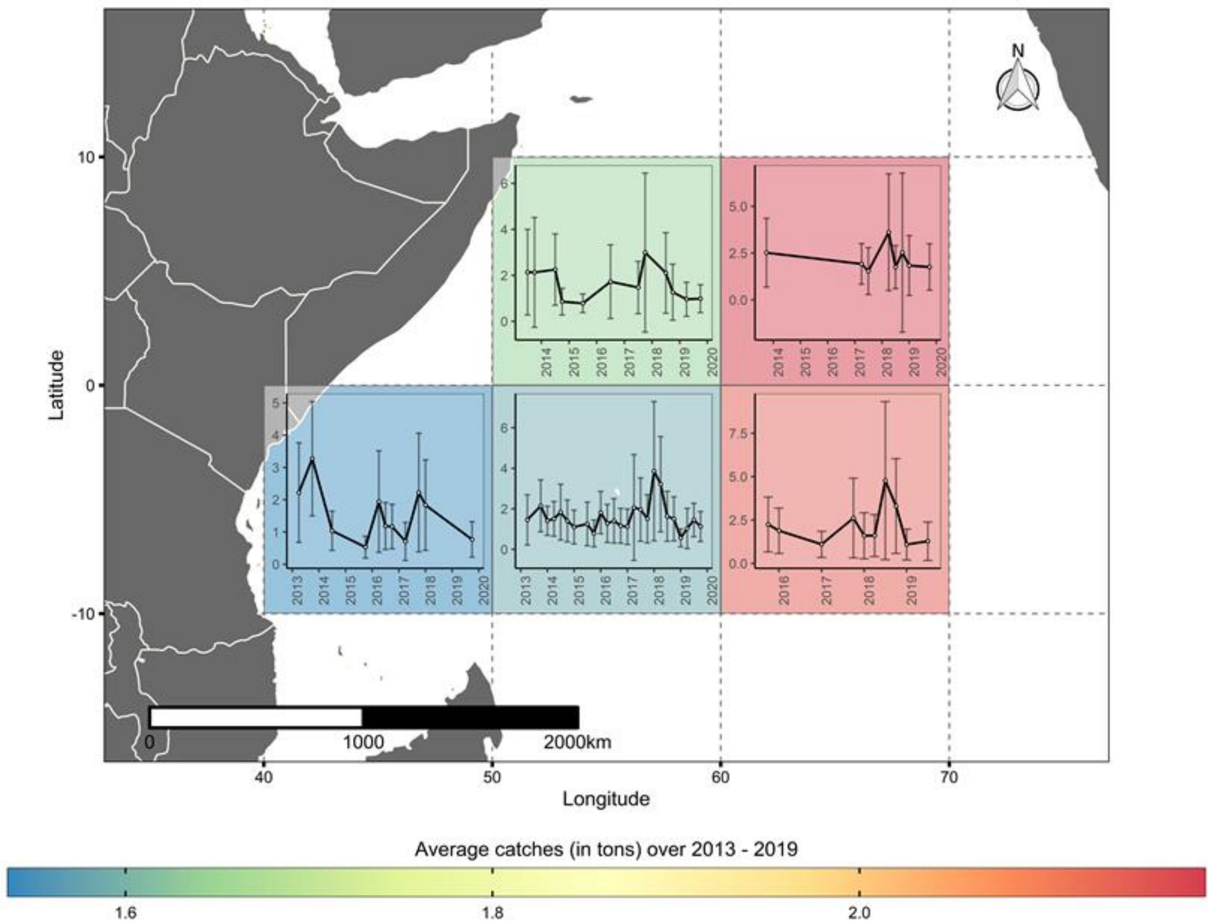

Figure 4: Quarterly averages of FOB-associated biomasses (in tonnes) of small bigeye tuna BET(<10kg) per FOB set by 10° × 10° spatial strata in the western Indian Ocean. The background colors indicate the average biomass calculated from 2013 to 2019 in each spatial stratum.

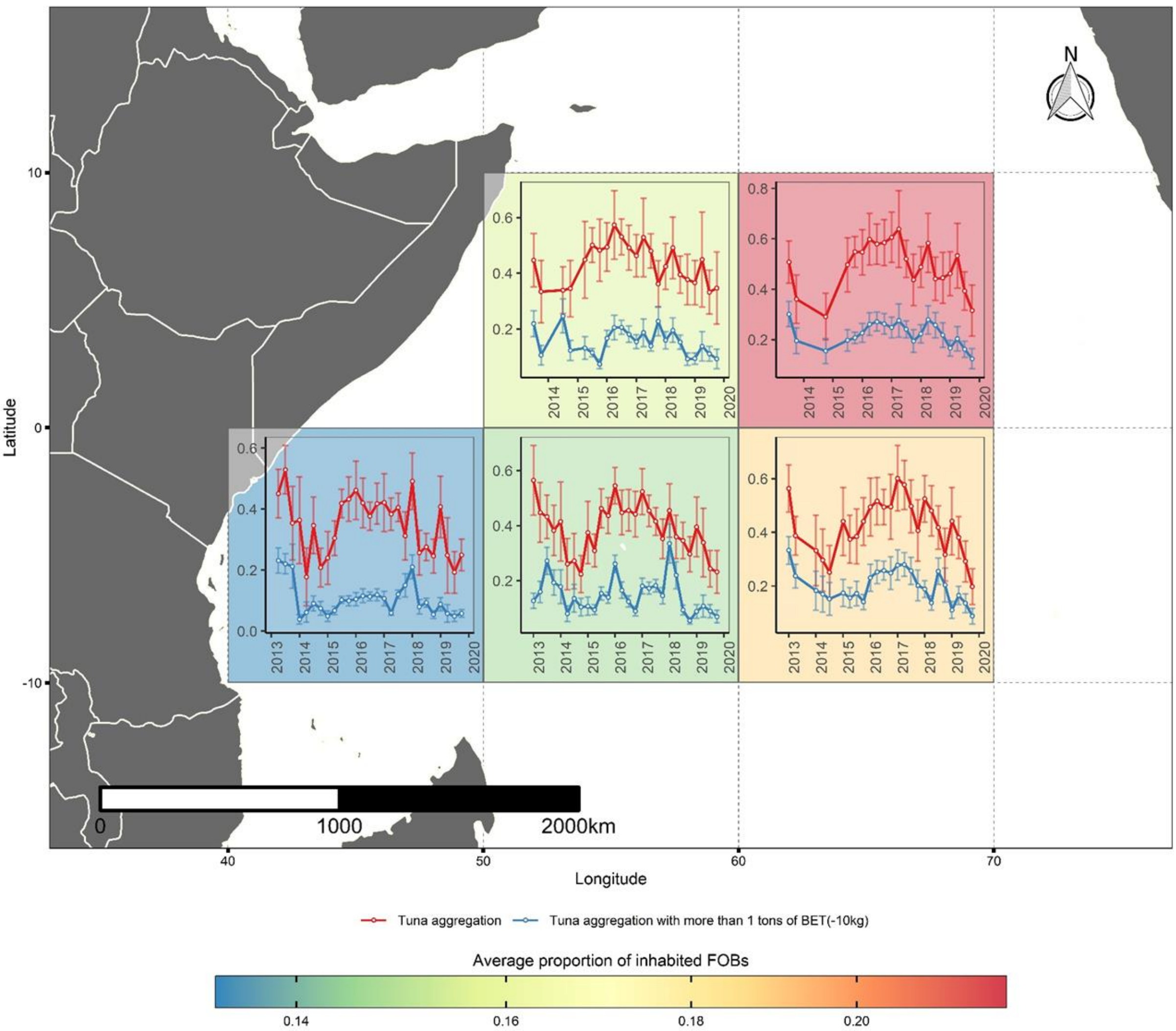

Figure 5: Quarterly averages of the daily proportion of FOBs inhabited by small bigeye tuna BET (<10kg) by 10°×10° spatial strata in the western Indian Ocean. The background colors indicate the average proportion of FOBs with tuna aggregations greater than 1 tonne (all three species) from 2013 to 2019 in each spatial stratum.

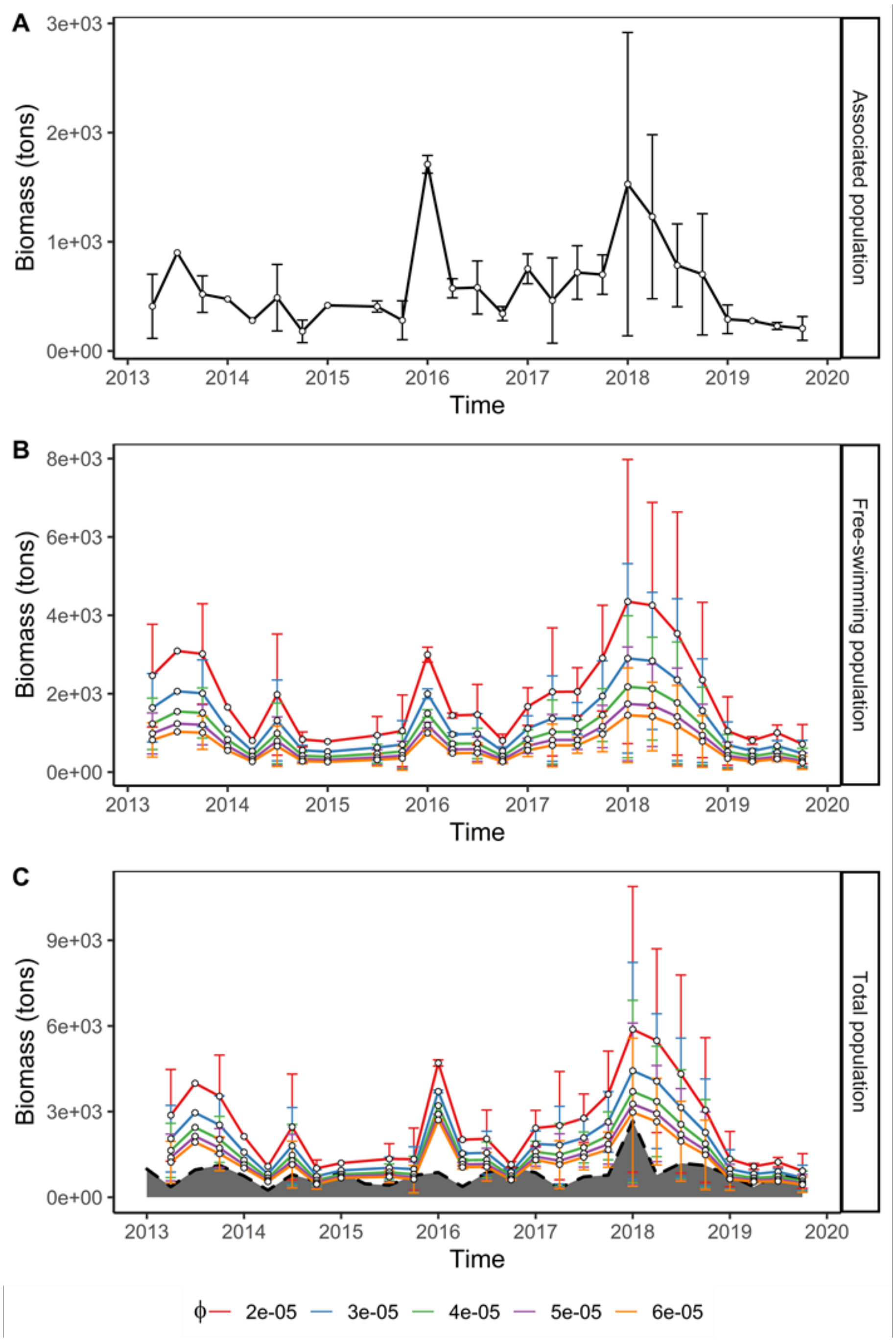

Figure 6: Absolute estimates of the Associative Behavior Based abundance Index (ABBI) for the different population component (associated and unassociated) of small bigeye tuna (<10 kg) in the western Indian Ocean. (**A**) Time series of the average absolute abundances of the associated component per 10° × 10° square. (**B**) Time series of the average absolute abundances of the unassociated component per 10° × 10° square, under different values of ϕ. (**C**) Time series of the average absolute abundances of the total population of small bigeye tuna (<10kg) per 10° × 10° square, under different values of ϕ. The shaded areas correspond to the average catches of small bigeye tuna (<10kg) per 10° × 10° square of all the fishing gears targeting the species in the western Indian Ocean.

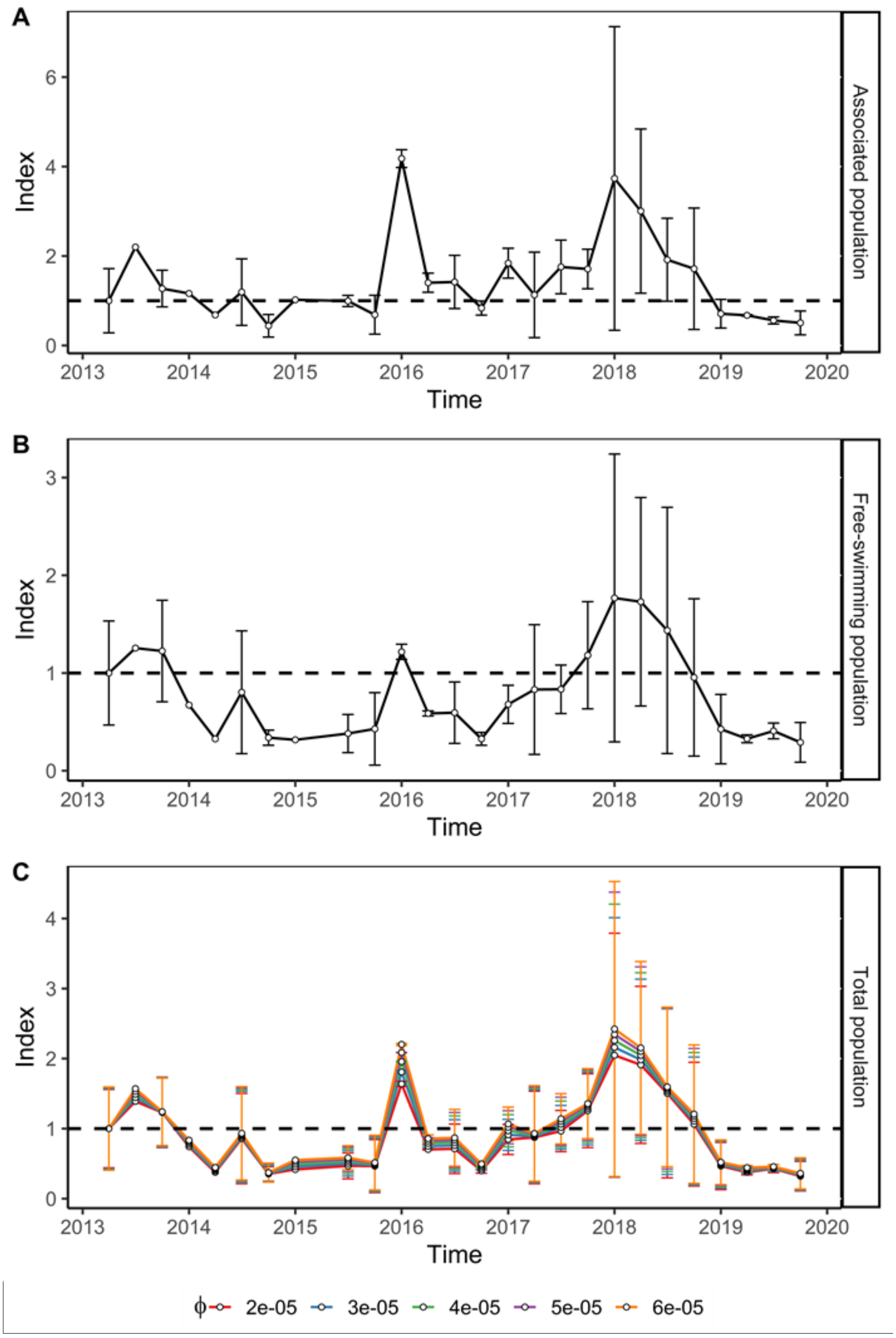

Figure 7: Relative estimates of the Associative Behavior Based abundance Index (ABBI) for the different population component (associated and unassociated) of bigeye tuna under 10 kg in the western Indian Ocean. (**A**) Time series of the relative abundances of the associated component. (**B**) Time series of the relative abundances of the unassociated component. (**C**) Time series of the relative abundances of the total population of small bigeye tuna (>10 kg), under different values of ϕ.